# Lawrence Berkeley National Laboratory
## Recent Work

**Title**

A GENERALIZATION OF THE PROXIMITY FORCE THEOREM

**Permalink**

https://escholarship.org/uc/item/12j7s7p8

**Author**

Blocki, J.

**Publication Date**

1980-08-01

# Lawrence Berkeley Laboratory
## UNIVERSITY OF CALIFORNIA

A GENERALIZATION OF THE PROXIMITY FORCE THEOREM

J. Blocki and W.J. Światecki

August 1980

NUCLEAR SCIENCE DIVISION

LBL-9574 c.2

## DISCLAIMER

# A GENERALIZATION OF THE PROXIMITY FORCE THEOREM

J. Błocki

Institute for Nuclear Research
05-400 Swierk, Poland

and

W. J. Świątecki

Lawrence Berkeley Laboratory
University of California
Berkeley, California 94720

## ABSTRACT

We generalize the Proximity Force Theorem of Ref. 1 (valid for

*gently curved* surfaces) to include surfaces that may have large curvatures

(but are still characterized by *small angles* between relevant portions

of the interacting surfaces). A general proof is given for the approxi-

mate continuity of the proximity force when a gap configuration goes over

into a crevice after contact. Simple and somewhat improved formulae are

given for the universal proximity potential functions $\Phi$ and $\hat{\Phi}$ for gaps

and crevices.

1.   INTRODUCTION

We shall describe a generalization of the Proximity Force Theorem derived in Ref. 1.  The generalization is important for discussing the interaction between types of surfaces for which the curvatures at the point of least separation are no longer small compared to the diffuseness of the surface region.  The derivation of the theorem is both more general and simpler than previous versions and can be used to obtain certain useful insights into the problem of approximating the energy of a thin-skinned (leptodermous) system, such as a nucleus, by a sum of a surface energy $V_S$ and a proximity potential $V_P$.

2.   THE SURFACE AND PROXIMITY ENERGIES

The potential energy of a configuration specified by a shape $\Sigma$ is written, approximately, as a constant volume energy and a shape-dependent part V, where

$$V = V_S + V_P \quad , \tag{1}$$

with

$$V_S = \gamma \iint_\Sigma d\sigma \quad , \tag{2}$$

$$V_P = \iint_{\substack{\text{gaps and} \\ \text{crevices}}} dx\,dy\; e(D) \quad . \tag{3}$$

In Eq. (2) $\gamma$ is the surface energy per unit area and the integration is over the surface $\Sigma$.  In Eq. (3) the additional interaction associated with gaps or crevices in $\Sigma$ is approximated as an integral over e(D), the interaction energy per unit area between plane, parallel

surfaces at the separation D. The integration is in the transverse x-y plane, at right angles to the line of least separation between the two pieces of $\Sigma$ specifying the gap or crevice.

The accuracy of the approximation underlying Eq. (3) depends on the smallness of the deviation from parallelism of the surface elements on the two sides of the gap or crevice. For gaps or crevices where the deviation from parallelism is not everywhere small, Eq. (3) may still be useful if the regions where the large deviations occur are sufficiently small or if the large deviations occur only outside the effective range of the function e(D).

The geometrical configurations that we shall consider will include cases in which the shape $\Sigma$ is in the form of a single object or of two (or more) pieces. In the latter case the two pieces may be separated by a gap, with a least separation s. We shall include in our discussion the case where s is negative, which means that the pieces have overlapped (and the density in the overlap region would eventually be doubled). We shall refer to such configurations (where the pieces are either separated or overlapping) as Gap configurations. In contrast, a configuration resulting from first overlapping two surfaces, erasing the overlapping portions and then filling the resulting single shape with matter, without any density doubling, will be called a Crevice configuration (see Fig. 1).

3. THE PROXIMITY THEOREM

The key trick of the Proximity treatment is the transformation of the two-dimensional integral in Eq. (3) into a one-dimensional integral as follows:

$$V_p = \int_{s \text{ or } 0} e(D) \, J \, dD \quad , \tag{4}$$

where $J$, the Jacobian of the transformation, is proportional to the area between two contours in the x-y plane corresponding to gap widths $D$ and $D + dD$:

$$J = \frac{d(\text{area in x-y plane})}{dD} \quad . \tag{5}$$

We shall refer to $J$ as the gap width distribution function. The significance of $J$ may be appreciated by an analogy. Imagine, instead of gap width contours in the x-y plane, a chart of depth contours of the central portion of a lake or reservoir, shallowest in the middle and getting deeper towards the edges. By plotting the area between successive depth contours as a function of the depth, one obtains a "depth distribution function" of the lake or reservoir, analogous to $J$. In the case of a gap the depth distribution starts with the least depth $s$, and the lower limit of integration in Eq. (4) is $s$. The case of negative s-values corresponds to a lake or reservoir with an island or boulder in the middle, the elevation contours of the island being counted as negative depths. In the case of a crevice these elevations are disregarded and the depth distribution function starts with the zero depth contour around the island's edge. The lower limit of integration in Eq. (4) is thus zero for crevices. The upper limit of integration may often be extended to infinity — but see Section 4.

It is clear that for given surfaces at varying separations the gap width distribution function is a function of the difference $D-s$ only,

and not of D and s separately. (We shall denote D-s by z). Thus,

$$V_p = \int\limits_{s \text{ or } 0} e(D) \, J(D-s) \, dD \quad , \tag{6}$$

where $J(z)$ is a function of the type illustrated in Fig. 2. It follows by differentiation that the proximity force between two surfaces is, for gaps

$$-\frac{\partial V_p^{gap}}{\partial s} = J_o e(s) + \int\limits_s e(D) J'(D-s) \, dD \quad , \tag{7}$$

$$\to J_o e(0) + \int\limits_0 e(D) J'(D) \, dD \quad \text{for } s \to 0 , \tag{7a}$$

and, for crevices

$$-\frac{\partial V_p^{crevice}}{\partial s} = \int\limits_0 e(D) J'(D-s) \, dD \tag{8}$$

$$\to \int\limits_0 e(D) J'(D) \, dD \quad \text{for } -s \to 0 . \tag{8a}$$

In the above, $J_o$ stands for $J(0)$ and $J'$ is the derivative of $J$.

We note the general result that the discontinuity in the proximity force as a gap turns into a crevice at s=0 is

$$\Delta_p \equiv \left( -\frac{\partial V_p^{gap}}{\partial s} \right)_{s=0} - \left( -\frac{\partial V_p^{crevice}}{\partial s} \right)_{s=0} = J_o \, e(0) \quad .$$

Now the discontinuity (at s=0) in the force due to the surface-energy part of the potential is

$$\Delta_S \equiv \left( -\frac{\partial V_S^{gap}}{\partial s} \right)_{s=0} - \left( -\frac{\partial V_S^{crevice}}{\partial s} \right)_{s=0} = 2\gamma J_o \quad .$$

This is because, from the definition of J, $2J_o(-ds)$ is the area of the
two infinitessimal caps of the overlapping pieces which are to be erased
when the overlap is (-ds), and this results in a saving in surface
energy equal to $2\gamma J_o(-ds)$. Note also that the derivative $\partial V_s^{gap}/\partial s$
is, of course, zero. The discontinuity in the *total* force is then

$$\Delta = J_o[e(0) + 2\gamma] \quad . \qquad\qquad (8b)$$

The value of e(0) is, from the definition of e(s), the interaction energy
per unit area between two juxtaposed flat surfaces at contact. In the
case of density distributions with "symmetric" fall-off profiles, such
that the sum of the densities at contact adds up to the constant standard
bulk density, the superposition of the densities results in the destruc-
tion of the two surfaces together with their associated surface energies,
so that $e(0) = -2\gamma$. This leads to the following general theorem:

> "The sum of the surface and proximity energies is continuous
> (in the first derivative) when a gap turns into a crevice
> at contact."

There are no restrictions on the gap geometry or the smallness of
the diffuseness (but the density fall-off profile *is* assumed to be
symmetric).

Coming back to Eqs. (7) and (8), we shall now introduce specific
assumptions about the appearance of J(D). First, if we assume that,
within the range of the function e(D), the gap width function may be
approximated by the constant $J_o$, Eqs. (7),(8) lead to the conventional
Proximity Force Theorem which states that the proximity force between
gently curved surfaces is proportional to the interaction energy per unit

area between flat surfaces, i.e., to the universal proximity force function $e(s)$, (and that for crevices the proximity force is zero). The factor of proportionality is $J_o$, which we shall call the curvature index of the gap between the surfaces. (It is equal to $4\pi$ times the mean curvature radius $\bar{R}$ [see Ref. 1, p.431].)

If we now make the more general assumption that, within the range of $e(D)$, the gap width function $J(D)$ may be approximated by a linear expression

$$J(D) \approx J_o + J_1 D \quad , \tag{9}$$

we may write

$$-\frac{\partial V_P^{gap}}{\partial s} \approx J_o e(s) + J_1 \&(s) \tag{10}$$

$$\rightarrow J_o e(0) + J_1 \&(0) \quad \text{for } s \rightarrow 0 \quad , \tag{10a}$$

and

$$-\frac{\partial V_P^{crevice}}{\partial s} \approx J_1 \&(0) \quad . \tag{11}$$

In the above, $\&(s)$, (the universal proximity potential function), is the following indefinite integral over $e(s)$ :

$$\&(s) = \int_s e(s) \, ds \quad , \tag{12}$$

and we shall refer to $J_1$ (the slope of $J(D)$) as the "Peaking Index" of the gap (see Section 4).

The generalized Proximity Force Theorem may now be stated as follows:

"The proximity force between two curved surfaces as a function
of the separation degree of freedom  s  is approximately equal
to the product of the geometrical curvature index $J_o$ of the

gap between the surfaces and the universal proximity force function e(s) (the interaction energy per unit area between flat, parallel surfaces), augmented by the product of the geometrical peaking index $J_1$ of the gap and the universal proximity potential function &(s) (an indefinite integral of e(s)). For crevices, the first term is absent and the second is a constant."

The total force (including that due to the surface energy) is now, for gaps

$$-\frac{\partial V^{gap}}{\partial s} = J_0 e(s) + J_1 \&(s), \tag{13}$$

and, for crevices with small overlaps,

$$-\frac{\partial V^{crevice}}{\partial s} \approx -2\gamma J_0 + J_1 \&(0). \tag{14}$$

Introducing the dimensionless quantities

$$\zeta \equiv s/b \quad, \tag{15}$$

$$\Phi(\zeta) \equiv \frac{1}{2\gamma b} \int_s e(s) \, ds \quad, \tag{16}$$

$$\Phi_1(\zeta) \equiv \frac{1}{2\gamma b^2} \int_s \&(s) \, ds \quad, \tag{17}$$

we may now write the total energy for a family of shapes that changes from a gap to a crevice at s=0 in the following form

$$V = 2\gamma b [J_0 \Phi(\zeta) + b J_1 \Phi_1(\zeta)] \qquad \text{for } \zeta \geq 0 \, , \tag{18a}$$

$$V \approx 2\gamma b [J_0 - J_1 b \dot{\Phi}(0)](\zeta - \zeta_c) \qquad \text{for } \zeta \leq 0 \, , \tag{18b}$$

where

$$\zeta_c \equiv \frac{s_c}{b} = \frac{J_0\Phi(0) + J_1 b\Phi_1(0)}{-J_0 + J_1 b\Phi(0)} \quad . \tag{19}$$

The universal functions $\Phi(\zeta)$, $\Phi_1(\zeta)$ were tabulated (for nuclear surfaces) in Ref. 1.

We note that in the case of a gap with a zero value of the peaking index $J_1$ (this corresponds to a paraboloidal gap [see Section 4]) which turns into a crevice for $s < 0$, the total energy may be written as

$$V = 2\gamma b J_0 \hat{\Phi}(\zeta) \quad , \tag{20a}$$

where

$$\hat{\Phi} = \Phi(\zeta) \qquad \text{for } \zeta \geqslant 0 \tag{20b}$$

$$\hat{\Phi} \approx \zeta - \zeta_c \qquad \text{for } \zeta \leqslant 0 , \tag{20c}$$

with

$$\zeta_c = -\Phi(0)$$

$$= 1.7817 , \text{ for nuclear surfaces.}$$

This function $\hat{\Phi}(\zeta)$ is plotted in Fig. 3 as the solid curve. For $\zeta \leqslant 0$, $\hat{\Phi}$ is a straight line with unit slope. For $\zeta \geqslant 2.74$ the function $\hat{\Phi}(\zeta)$ (the same as $\Phi(\zeta)$) is a pure exponential with a range 0.7176 (see footnote to Table I in Ref. 1). Approximating $\hat{\Phi}$ (or $\Phi$) in the interval $0 \leqslant \zeta \leqslant 2.74$ by a continuation of this exponential down to $\zeta = 1.9475$, joined smoothly to a cubic with value and slope at $\zeta = 0$ matching the exact Thomas-Fermi function $\Phi$, results in the following formulae:

$$\hat{\Phi} = \Phi \approx -4.41 \, e^{-\zeta/0.7176} \quad , \qquad \text{for } \zeta \geqslant 1.9475$$

$$\text{(exact for } \zeta \geqslant 2.74), \tag{21a}$$

$$\hat{\Phi} = \Phi \approx -1.7817 + 0.9270\zeta + 0.01696\zeta^2 - 0.05148\zeta^3,$$

$$\text{for } 0 \leqslant \zeta \leqslant 1.9475 \quad (21b)$$

$$\hat{\Phi} = -1.7817 + \zeta \quad , \quad\quad\quad \text{for } \zeta \leqslant 0 \quad . \quad\quad (21c)$$

Also shown in Fig. 3 (as a dashed line) is a continuation of $\Phi$ to negative gap configurations, i.e., to overlapped systems with doubled densities. A cubic approximation to this part of $\Phi$ is

$$\Phi \approx -1.7817 + 0.9270\zeta + 0.143\zeta^2 - 0.09\zeta^3 \quad , \quad \text{for } \zeta \leqslant 0 \quad . \quad\quad (21d)$$

Equations (21a-21d) give useful approximations to the gap function $\Phi$ and the gap-crevice function $\hat{\Phi}$ (see the circled points in Fig. 3). They are somewhat preferable to the "cubic-exponential" approximation (Eq. (27) in Ref. 1) in that they reproduce the Thomas-Fermi values *exactly* for $\zeta \geqslant 2.74$ and are continuous (to within a few units in the fifth decimal) in value, slope *and* second derivative at the junction point $\zeta = 1.9475$.

A rough straight-lines approximation to $\hat{\Phi}$ is:

$$\hat{\Phi} \approx 0 \quad\quad \text{for } \zeta \geqslant \zeta_c \quad ,$$

$$\hat{\Phi} \approx \zeta - \zeta_c \quad \text{for } \zeta \leqslant \zeta_c \quad ,$$

where

$$\zeta_c = 1.7817 \approx \sqrt{3} \quad .$$

This is a very poor approximation in the tail (see the dotted lines in Fig. 3) but, because of its simplicity, is still of some use in semi-quantitative studies of nuclear collision dynamics (see Ref. 3).

The gap function $\Phi(\zeta)$ is sometimes referred to as *The* Proximity Theorem prediction for the interaction potential between nuclei. It

needs to be stressed again that whether one uses the gap function $\Phi(\zeta)$ or the crevice function $\hat{\Phi}(\zeta)$ for negative $\zeta$ depends on whether one believes the physical situation in question to be better approximated by a pile-up of density in the overlap region or a redistribution of the density to a nearly uniform value. For high-energy nucleus-nucleus collisions the former situation might be relevant, but for low-energy collisions it is surely on the latter that one should focus one's attention. ("High" and "low" means collision energies per nucleon high or low compared to typical Fermi-motion energies in the colliding nuclei, some 20 MeV in order of magnitude.) But even $\hat{\Phi}$ is expected to become less and less relevant as the neck or window between the two colliding systems opens up beyond the "geometrical" value defined by the intersection of the two overlapping surfaces describing the original nuclei. The opening up of the neck beyond the geometrical value would, in fact, be expected to result in a further saving in surface energy and a lowering of the potential below the estimate provided by using the function $\hat{\Phi}(\zeta)$. With the neck degree of freedom included, the potential energy is no longer a function of a single separation variable (s or $\zeta$) and a map of V in at least two dimensions is required. Suitable proximity corrections may still be used in such cases to improve the estimate of the nuclear potential corresponding to a sum of volume and surface energy terms (see Refs. 1 and 3).

Figure 4 shows how the (almost) smooth interaction function corresponding to $\hat{\Phi}$ is made up of the surface energy and the proximity energy, each of which has a marked discontinuity in the first derivative. The example corresponds to two equal paraboloids with tips characterized

by a radius of curvature $R$, equal to five times the surface width $b$.
(The reduced radius of the gap is thus $\bar{R} = 2.5b$.)

Figure 5 is a similar analysis of the potential energy for two
equal spheres. There are again marked discontinuities in the slopes
of $V_S$ and $V_p$ as the gap turns into a crevice at contact but the sum, $V$,
is (nearly) smooth. (Only "nearly" because the interaction function
$e(D)$ underlying these examples is based on a Thomas-Fermi model of the
surface for which $e(0)$ differs from $-2\gamma$ by 7.3% and this leads to an
imperfect cancellation between $e(0)$ and $2\gamma$ in Eq. (8b).)

In Fig. 6 the interacting surfaces are equal circular cones with
semi-opening angles of 60°. In this case all the curves $V_S$, $V_p$ and $V$
have continuous first derivatives.

In all these figures the energies are in units of $2\gamma b^2$ (roughly
2 MeV) and the separation $s$ is in units of $b$ (roughly 1 fm).

4.    THE GAP WIDTH DISTRIBUTION FUNCTION $J(z)$

In Fig. 2 we have plotted $J(z)$ for gaps corresponding to the
following surfaces:  a) two equal paraboloids,  b) two equal spheres,
c) two unequal spheres,  d) a sphere and a plane,  e) two equal hyperbol-
oids,  f) two equal cones.  Because $J$ is the only information about the
interacting surfaces that enters into the proximity potential, Eq. (4),
this potential is invariant with respect to deformations of the interact-
ing surfaces that preserve the areas $Jdz$ between successive width
contours. The variety of interacting surfaces that are all characterized
by the same width distribution function may be appreciated by the
following construction. Imagine a set of width contours drawn on a

sheet of thick rubber representing the x-y plane, a series of holes made along each contour labeled by D, and a set of rods of length D inserted normally into the holes. The two ends of the rods may be imagined as defining the two interacting surfaces. Starting with these surfaces we may now generate a host of new surfaces by: a) stretching the rubber sheet according to transformations that preserve the areas between successive width contours, b) sliding the rods in their holes according to arbitrary prescriptions, and c) bending the rubber sheet (slightly). The multitude of surfaces generated in this way have clearly the same gap width distribution function and would be characterized by the same proximity interaction.

In connection with Fig. 2, note that in the case of paraboloids, hyperboloids or cones, J is a single-valued function extending to infinite values of the argument z, and the proximity integral in Eq. (4) remains well-defined when the upper limit of integration is extended to infinity. In the case of a sphere R and a plane, the function J turns negative at z=R and would continue to z = 2R, where it would stop altogether: there are no gap widths greater than the diameter 2R augmented by the separation s. In this case the extension of the integral in Eq. (4) to infinity would include an unphysical contribution from z > 2R. The contribution from the interval R < z < 2R, where J is negative, subtracts the interaction between slabs whose separations correspond to the distances between the plane and the *back side* of the sphere. The effect is, qualitatively at least, in the sense of recognizing the finite thickness of the sphere. Thus a proximity integral extended to D = 2R + s would correspond to the replacement of the interaction between a plane and a sphere by an integral over interactions per unit area of

a plane and a series of *slabs*, whose finite thicknesses were matched
appropriately to the chords of the sphere. Formally the gap width D is,
in this case, a double-valued function of x,y (even though J(z) remains
single-valued). In the case of unequal spheres there are *four* distances
between the front and back parts of the spheres and the interaction
could be approximated by an integration over interactions per unit area
of two finite slabs. Finally, one could formally recognize the front
and back surfaces of a *single* sphere as associated with an interaction
between negative (missing) semi-infinite slabs that have to be removed
in order to convert infinite nuclear matter into a sphere of finite
dimensions. The proximity integral for two unequal spheres would then
involve *six* gap widths for each given x,y. Two of the gap widths would
be associated with the self-energies of the spheres. These would be
constant for separated spheres (and would not affect the force between
them), but would become functions of the overlap for crevices. The
effects associated with these generalizations are small so long as the
sizes of the objects in question are large compared to the range
of the interaction function e(D). We have not pursued their analysis
to a stage where we felt that it would be useful to retain them
without including other corrections that might be equally important.

Figure 2 illustrates the importance, in certain situations, of the
present generalization of the Proximity Force Theorem. Thus for hyperbol-
oidal surfaces the curvature index $J_o$ may become very small or even zero as
the hyperboloids degenerate into cones. The standard Proximity Theorem
would then give the (useless) prediction of a zero force between such
surfaces, whereas the generalized theorem would give a finite answer that

would, in fact, be accurate provided only the angles between the interacting surfaces were not too large (but with no restrictions on the curvature at the tips).

We have called the slope $J_1$ of the width distribution function the "Peaking Index" of the gap because it distinguishes between functions such as a conical volcano peak (with positive $J_1$), a paraboloidal sugar-loaf mountain (with $J_1=0$), and an even less peaked hemispherical boulder (with negative $J_1$).

Note finally that even complicated, multiply-connected width contour patterns may have simple width distribution functions (that can be approximated by expressions of the form $J \approx J_0 + J_1 D$). Thus in the discussion of the cohesive forces between *rough* surfaces one might find it useful to approximate the gap by an infinite array of a mixture of spherical, paraboloidal, cylindrical, hyperboloidal or conical protrusions, all of which would lead approximately to gap width distribution functions of the above type.

REFERENCES

1.  J. Błocki et al., Annals of Phys. <u>105</u> (1977) 427.

2.  J. Randrup, Nucl. Phys. <u>A307</u> (1978) 319.

3.  W. J. Świątecki, "Three Lectures on Macroscopic Aspects of Nuclear
    Dynamics," International School of Nuclear Physics, "Ettore Majorana"
    Center for Scientific Culture, Erice-Trapani, Sicily, March 26 -
    April 9, 1979, Progr. in Particle and Nucl. Physics <u>4</u> 383 (1980);
    Lawrence Berkeley Laboratory Preprint LBL-8950 (March 1979).

FIGURE CAPTIONS

Fig. 1.  Schematic illustration of a Gap and a Crevice.  In the case of
         a gap, the least separation  s  may be positive or negative,
         the latter corresponding to overlapping objects.  In the case of
         a crevice,  s  is negative but the density is uniform throughout
         the single object (apart from a small diffuseness of the surface).

Fig. 2.  Examples of the width distribution function  J  (in units of $2\pi b$)
         for a) two equal paraboloids,  b) two equal spheres,  c) two
         unequal spheres with a 2:1 ratio of radii,  d) a sphere and a
         plane,  e) two equal hyperboloids with asymptotes at $60°$,
         f) two equal cones with semi-opening angle $60°$.  The curvature
         index $J_0$ was chosen to be the same in cases a-d, and corresponds
         to the value of $J_0$ for two equal spheres with radii five times
         the surface width  b.  The plot is against  z'(the gap width D
         less the least separation  s) in units of  b.  Only in the case
         of unequal spheres is the approximation  $J \approx J_0 + J_1 z$  not exact.

Fig. 3.  The universal potential energy function $\Phi(\zeta)$ (for a gap) and
         $\hat{\Phi}(\zeta)$ (for a gap that turns into a crevice when $\zeta < 0$).  The
         dashed and solid curves correspond to the exact Thomas-Fermi
         results and the circled points to cubic approximations for
         $\zeta \leq 1.9475$ and to an exponential for $\zeta \geq 1.9475$ (which becomes
         exact for $\zeta \geq 2.74$).  The dots indicate a super-simple straight
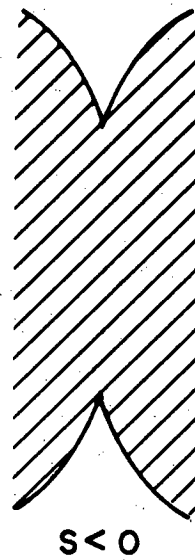         lines approximation to $\hat{\Phi}(\zeta)$.

Fig. 4.  The surface, proximity and total energies ($V_S$, $V_p$ and V) for a

paraboloidal gap that turns into a paraboloidal crevice when

the separation s is negative.  The gross discontinuities in

the slopes of $V_S$ and $V_p$ at s=0 almost cancel in the sum V by

virtue of Eq. (8b).  The mean curvature radius $\bar{R}$ in this example

is 2.5 times the surface width b  (b $\approx$ 1 fm).  The energy unit

is $2\gamma b^2$ (about 2 MeV).


Fig. 5.  Same as Fig. 4, but for two equal spheres with radii five times

the surface width b.


Fig. 6.  Same as Figs. 4 and 5 but for two equal cones with semi-opening

angle 60°.  In this case all the slopes are continuous at s=0.
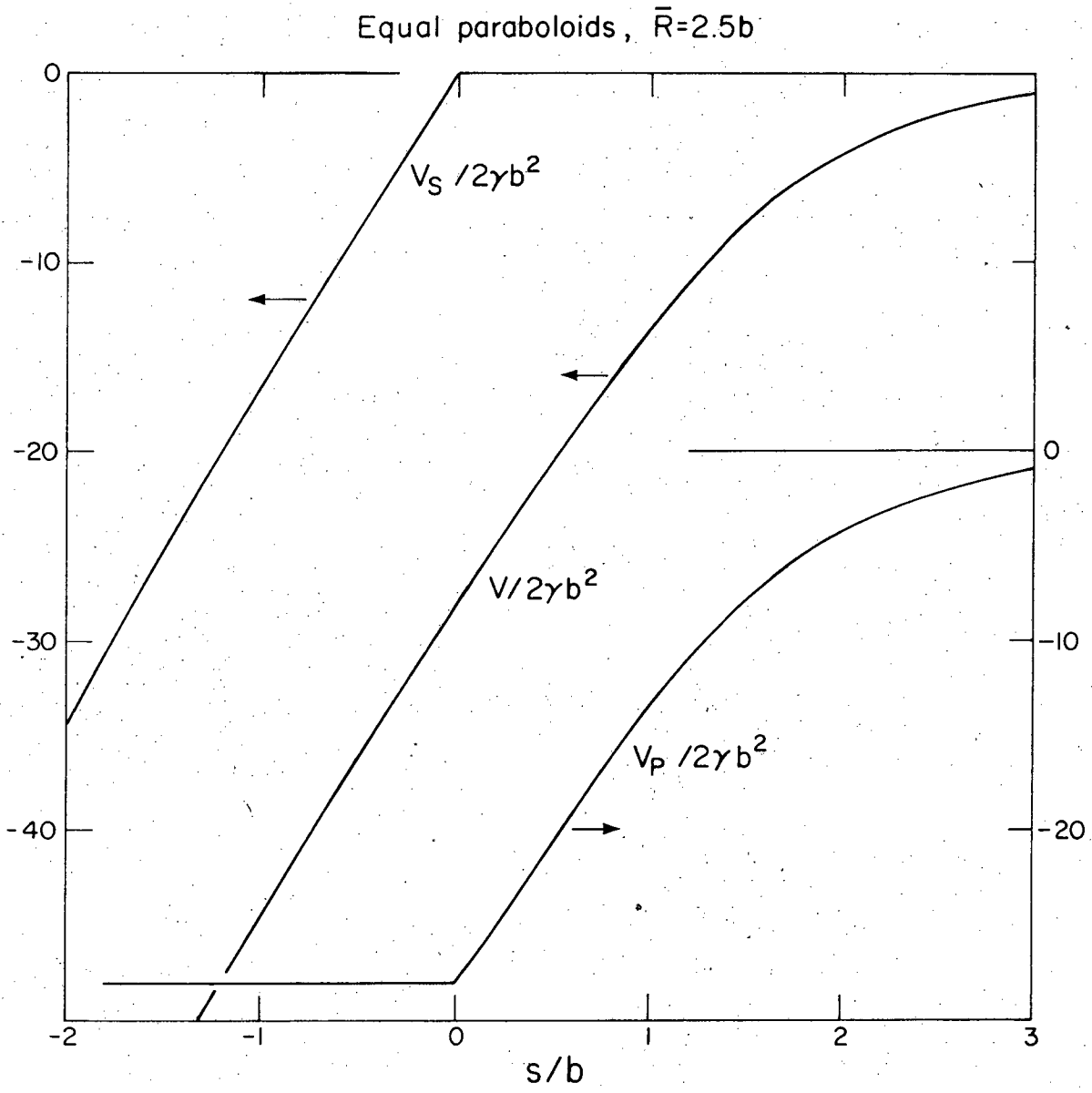
s > O              s < O

Gap

s < o
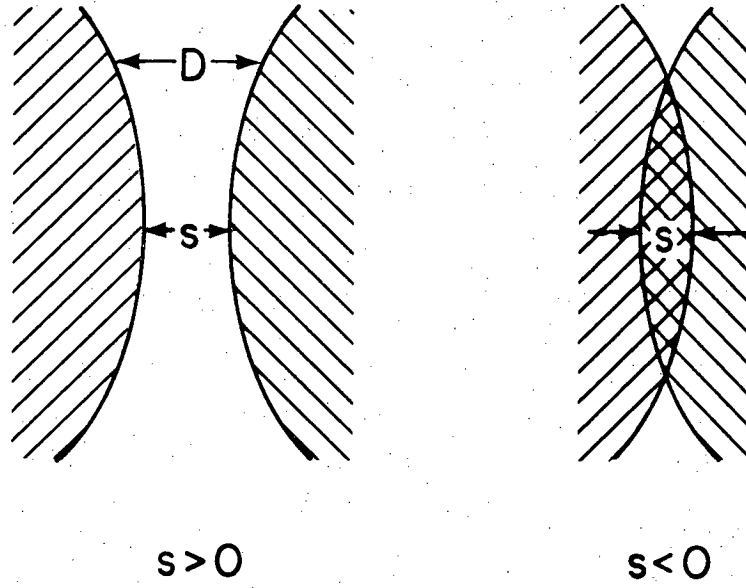
Crevice

XBL 7910-4364

Fig. 1

Fig. 2

Fig. 3

$\zeta$, The separation s in units of b

$\Phi$ and $\hat{\Phi}$, The Universal Potential Energy Functions in units of $2\gamma b^2$

$\zeta = 2.74$

$\zeta = 1.9475$

$\Phi(\zeta) = \hat{\Phi}(\zeta)$

$\hat{\Phi}(\zeta) = \zeta - 1.7817$

$\Phi(\zeta)$

XBL 7910 - 4369

Fig. 4

XBL 7910-4374

Equal spheres , R=5b
($\bar{R}$ = 2.5 b)



$V_S$ /2$\gamma b^2$

$V$/2$\gamma b^2$

$V_P$ /2$\gamma b^2$

s/b
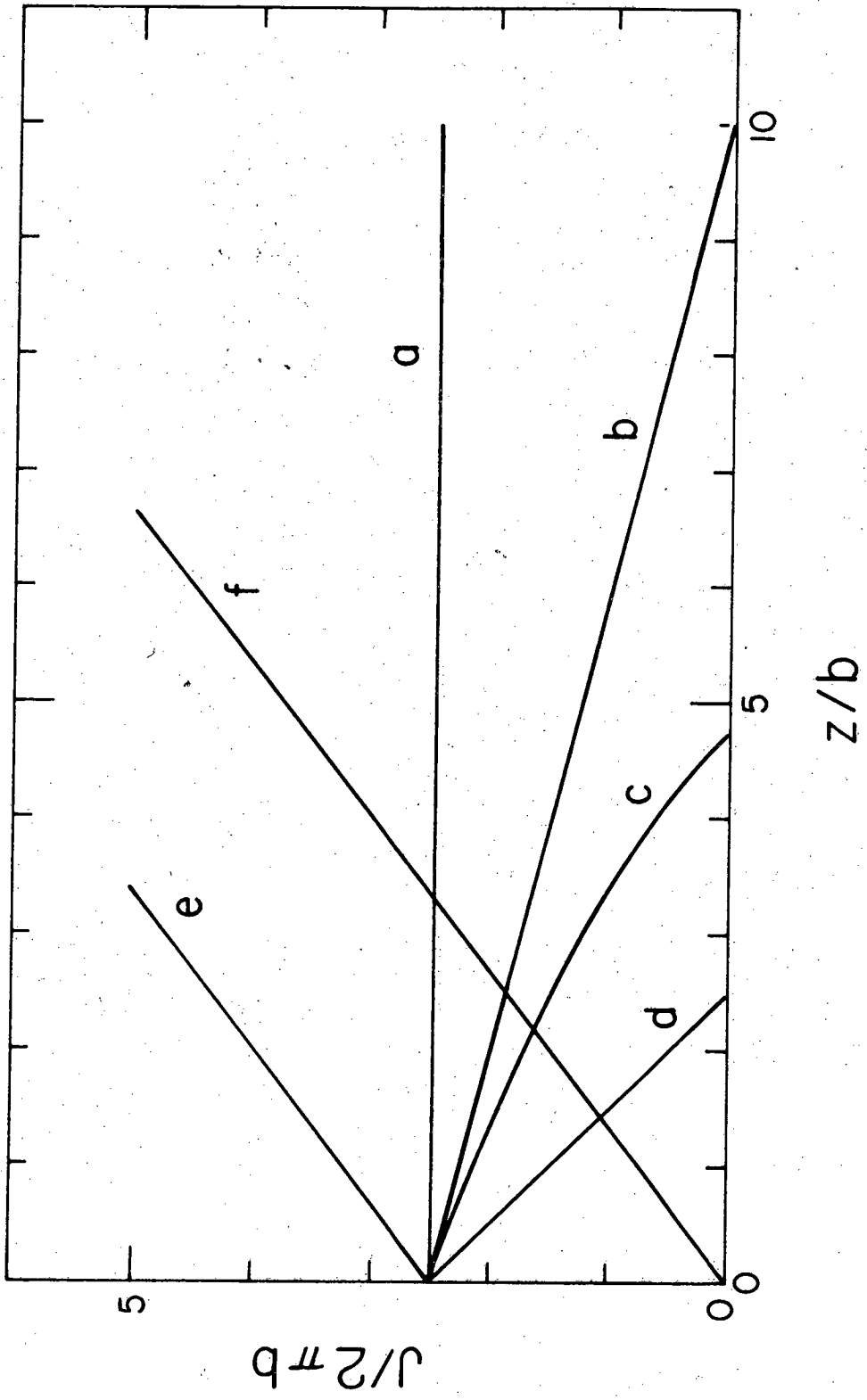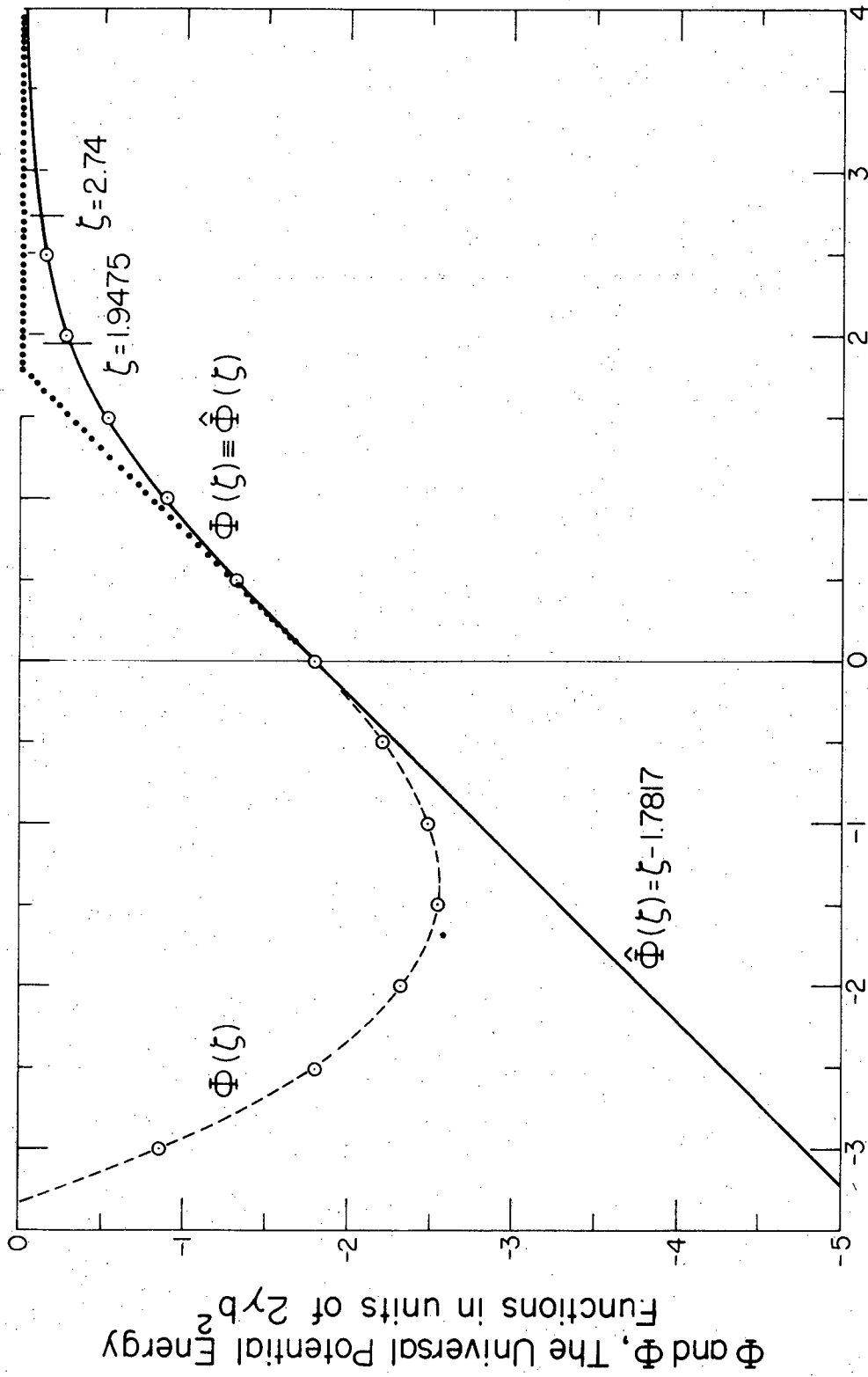
XBL 7910-4367

Fig. 5

Equal cones, $\alpha = 60°$

Fig. 6

XBL 7910-4373